RESEARCH NOTE

INVESTIGATION OF WAGON DERAILMENT MOVING ON RANDOM RAIL IRREGULARITIES USING NONLINEAR 3-DIMENTIONAL MODEL

M. Durali* and M.M. Jalili

Department of Mechanical Engineering, Sharif University of Technology
Center of Excellence in Design, Robotics and Automation
P.O. Box 11365-9567, Tehran, Iran
durali@sharif.edu – mmjalili@mehr.sharif.edu

*Corresponding Author

(Received: January 11, 2007 – Accepted in Revised Form: May 9, 2008)

Abstract Rail irregularity is one of the most effective factors in train derailment. theste irregularities have generally random distribution that are assumed to be stationary random and ergodic processes in space, with Gaussian amplitude probabiliy densities and zero mean values. The quality of irregularities, their distribution along the rails and wagon speed are the main factors for train derailment which is investigated in this article. The car model is nonlinear and three-dimensional with 48 DOF. Using simulation results, the safe speed for moving wagon on different types of random rail irregularities is also determined.

Keywords 3-D Train Model, Nonlinear Train Model, Random Rail Irregularities, Derailment, Simulation

چکیده ناهمواری های موجود روی ریل، یکی از عوامل مهم خروج قطار از خط هستند. این ناهمواری ها عموماً توزیع اتفاقی دارند و به وسیله یک تابع توزیع گوسی با مقدار متوسط صفر مدل می‌شوند. کیفیت و نحوه توزیع ناهمواری ها در دو ریل و همچنین سرعت عبور واگن بر روی ریل از عوامل مهم تأثیرگذار بر خروج از خط محورها است که در این مقاله به آنها پرداخته شده است. مدل واگن در این تحقیق مدلی سه بعدی و غیر خطی با ٤٨ درجه آزادی می‌باشد که تمام جزئیات واگن در آن لحاظ شده است. با استفاده از نتایج این بررسی، سرعت ایمن واگن در حالات مختلف حرکتی تحت تأثیر ناهمواری های اتفاقی تعیین شده است.

1. INTRODUCTION

Studies show that insufficient railway maintenance, train collisions, severe braking, passing over zigzag or curved routs, vertical and lateral rail irregularities are the main causes of train derailments. Various criteria have been used to predict the onset of derailment. One of these parameters is derailment coefficient which is defined as the ratio of lateral to vertical load at the wheel-rail contact point (Q/P). In 1908, Nadal, et al put forward the first equation to calculate the critical derailment coefficient [1]. Figure 1 shows the system of forces acting on the flange contact point. Using this figure, it can be written:

$$\frac{Q}{P}=\frac{\tan\alpha-(T/N)}{1+(T/N)\tan\alpha} \quad (1)$$

As tangential force T cannot exceed the value of normal force multiplied by dynamic coefficient of friction at wheel-rail contact point, the lower limit of derailment coefficient proposed by Nadal can be written as follow:

$$\frac{Q}{P}=\frac{\tan\alpha-\mu}{1+\mu\tan\alpha} \quad (2)$$

In Equation 2 μ is the dynamic coefficient of friction at wheel-rail contact point.

Although the derailment coefficient proposed

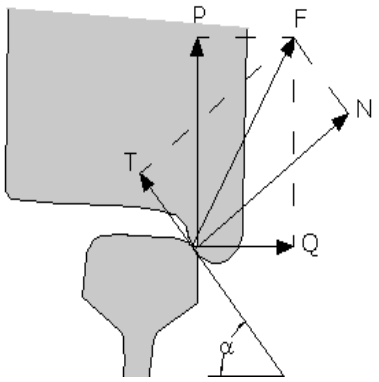

Figure 1. Forces acting on the wheel in wheel-rail contact point.

by Nadal is rather conservative, but due to its simplicity, it is still widely used. This coefficient determines the minimum value of Q/P at which a flange may climb the rail, causing derailment. Other criteria like equations proposed by Charter, et al [2] and Weinstock, et al [3] were also developed to investigate derailment theoretically. Weinstock's proposed criterion sets a limit on the sum of the absolute values of the derailment coefficients of the two wheels on a common axle. This is presented in the following equation:

$$\frac{Q}{P}=\frac{\tan\alpha\ (1+\mu^2)}{1+\mu\tan\alpha} \tag{3}$$

Although there are a number of such relations, for determining derailment coefficient theoretically, in many standards, the two quantities; Q and P, are measured experimentally or calculated by simulations to determine derailment coefficient. To determine Q and P by simulation, having an accurate dynamic model of train is essential.

Another index is the percentage of the wheel load reduction, $\Delta P/P_0$ in which P_0 is the wheel static load and ΔP is the reduction in the wheel static load in a dynamic situation. Limiting value for these characteristic differs with different standards. According to British standard, the value of Q/P when sustained for 0.05 seconds or more must not exceed 1.2. In addition vertical wheel load must never be less than 60 % of the static wheel load [3]. This standard can be expressed as follow:

$$\begin{cases}\dfrac{\Delta P}{P_0}<0.6\\ \dfrac{\Delta P}{P_0}=\dfrac{(P-P_0)}{P_0}\end{cases} \tag{4}$$

In Japanese standards, the maximum value of derailment coefficient is defined as follows [2]:

$$\begin{cases}\dfrac{Q}{P}=0.8 \quad \Delta t>0.05\,s\\ \dfrac{Q}{P}=\dfrac{0.04}{\Delta t} \quad \Delta t<0.05\,s\end{cases} \tag{5}$$

In which Δt denotes the time interval of maximum of Q/P.

In China railway, limiting value of Q/P is 1 and in north America 0.6 has been reported for maximum value of this ratio [4].

Simulation results with 2-dimensional wagon models indicate that normal force decrease in wheel-rail contact point for a wagon moving on random rail irregularities. Most 2-dimensional models for investigation of wheel-rail contact forces consider only vertical dynamics of wagon. As an example a combined rail-wagon model was introduced by Zhai, et al and Sun, et al, to determine vertical wheel-rail contact forces [5]. Similar model is developed by Sun and Dhanasekar to investigate vertical interaction of the rail track and the wagon system due to wheel and rail defects [6]. The wagon in later models have 10 degrees of freedom. The most complete 2-D, wagon models to investigate wagon response to random rail irregularities is used by references [7,8]. Au et al used a finite element 10 DOF wagon model to study the impact in cable-stayed railway bridges due to random rail irregularities [7]. They investigated the effects of line grade and wagon speed on bridge vibrations. Lei, et al and Noda, et al developed a finite element model to analyze the dynamic response of a vehicle and track coupling system excited by random vertical profile irregularities of the track for different speeds and line grades [8]. Simulation results have shown that normal forces in wheel-rail contact point is very sensitive to train speed and line grade. Also, Durali, et al and Jalili, et al showed that when wagon moves in high speed on low quality rail, separation between wheel and rail may occur [9].

Considering the nature of derailment, the use of 3-dimensional wagon model is essential. Determination of the correct contact point between wheel-rail and the exact value of the contact force between the two members are the major issues in 3-D modeling of derailment. There are two methods for deriving axle equations and determining contact forces between wheel and rail. In one method, the constraints against axle motion by the rail are used to calculate the normal forces at wheel rail contact point. This method was used by Durali and Shadmehri in dynamic study of train in sever braking [10]. In this reference, the yaw rotation of wheelset is neglected and so wheelset model has been reduced to a 2-D model. This method was also used to simulate the train in passing trough sharp bends [11]. Also using this approach an algorithm for solving the multibody differential and algebraic equations of the contact problem was presented by Shabana, et al [12].

The other method to determine wheel-rail contact parameters uses elastic contact theory of wheel and rail. In this method after determining the relative position of the wheel and the rail, Hertz contact theory is used to find the normal contact force between the two elements. The studies using this method are mostly two-dimensional and usually assume that the contact between wheel and the rail take place at the lowest point of the wheel. Some of these wheelset models have been presented in references [5-9].

There are also 3 dimensional models which have used this approach. For example, Shabana and Zaazaa have used a 3-D wheelset model to investigate lateral stability [13,14]. Also in these articles the results of the elastic methods are compared with the method of constrains. In addition, Durali and Jalili have used a 3-D wheelset model with 6 DOF to Investigate the effects of rail wear on derailment of the axle in passing over rail irregularities [15].

In the current article, the effects of random rail irregularities on wagon derailment are investigated, and the simulations are performed for different line grades.

Different factors such as unequal wheel load to each rail, wheel defect or creepage, inappropriate foundation, asymmetric rail wear and wheelset derailment cause dissimilar rail irregularities in right and left rails. Therefore, in this paper simulation is performed for both similar and dissimilar rails irregularities. Using the simulation, derailment coefficient and normal force in wheel-rail contact points, and wagon acceleration have been computed for all cases.

Usual experimental method for determining trains' safe speed involve much time and money. In current paper, a new method for determining allowable wagon speed for a wagon moving on randomly irregular rail track is presented and the simulation results are compared with federal railway administration (FRA) experimental results. A 3-D nonlinear wagon model that contains wagon body, bolsters, bogies and wheelsets is used for derailment simulations.

2. WAGON MODL

A 3-D model of a passenger wagon with 48 DOF is developed here. All parts of primary and secondary suspension systems with their nonlinear characteristics, friction between moving elements, the effect of wheel flange contact with the rail, wheel rail nonlinear contact forces, kinematics constraint of bogie center plate, the contact forces between side pads and bogie frame are considered in this model. A schematic of wagon models are shown in Figures 2 and 3.

References for these figures and the degrees of freedom for model components are listed in Table 1.

The wheels are connected to the bogies via primary suspension system and the bogies are connected to the wagon body through secondary suspension system. In this model, all clearances and nonlinearities in a real suspension system are considered.

Figure 4 represents the springs and damper forces as a function of relative displacement and velocity between the wagon components. The parameters for springs and dampers are presented in reference to [10].

The other source of nonlinearity in vehicle suspension is the coulomb friction between sliding surfaces. A mathematical representation of an ideal coulomb friction element is shown in Figure 5-a. in order to simulate coulomb friction, a small velocity region about the origin is included in which friction force will take values less than the break

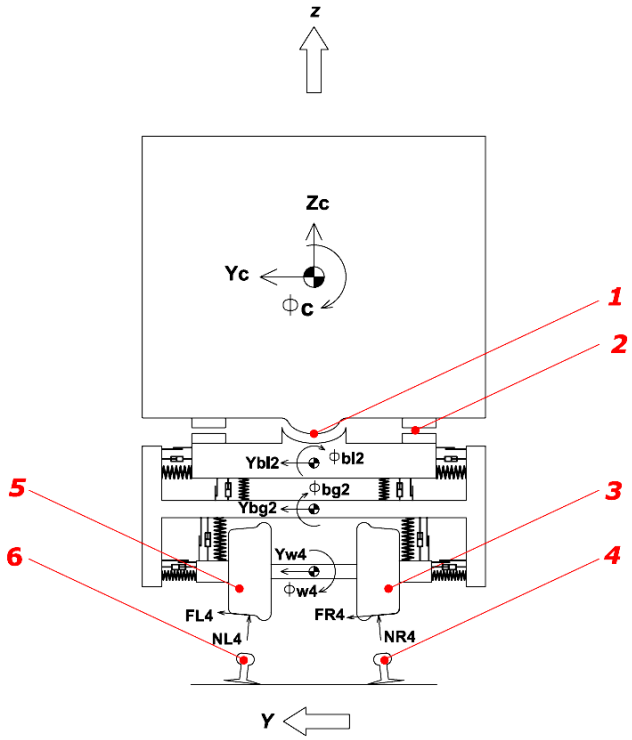

Figure 2. Front view of wagon model: (1) Centerplate, (2) Side pads, (3) Right wheel, (4) Right rail, (5) Left wheel, (6) Left rail.

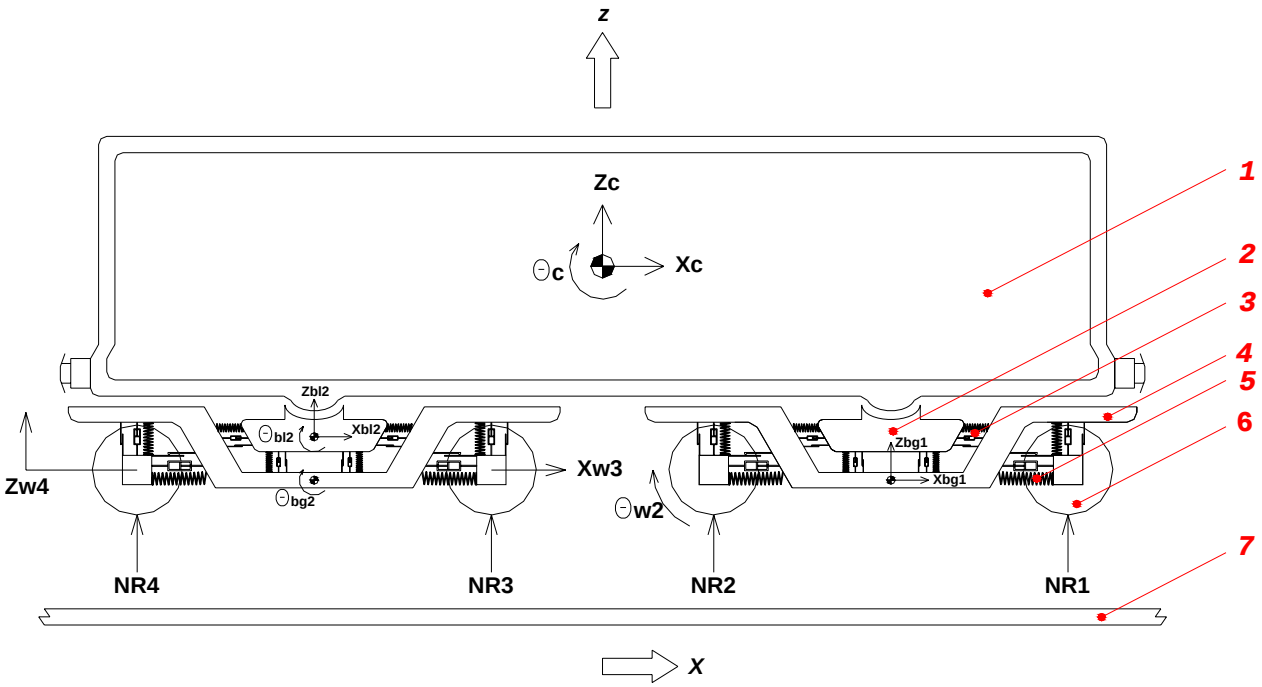

Figure 3. Side view of the wagon model: (1) Wagon body, (2) Bolster, (3) Secondary suspension system, (4) Bogie, (5) Primary suspension system, (6) Wheelset, (7) Rail.

TABLE 1. Degrees of Freedom of Each Part of the Model.

Component	Number	DOF	Total DOF
Wheel Sets	4	6	24
Bogie Frame	2	6	12
Bolster	2	3	6
Wagon Body	1	6	6
Total Degrees of Freedom			48

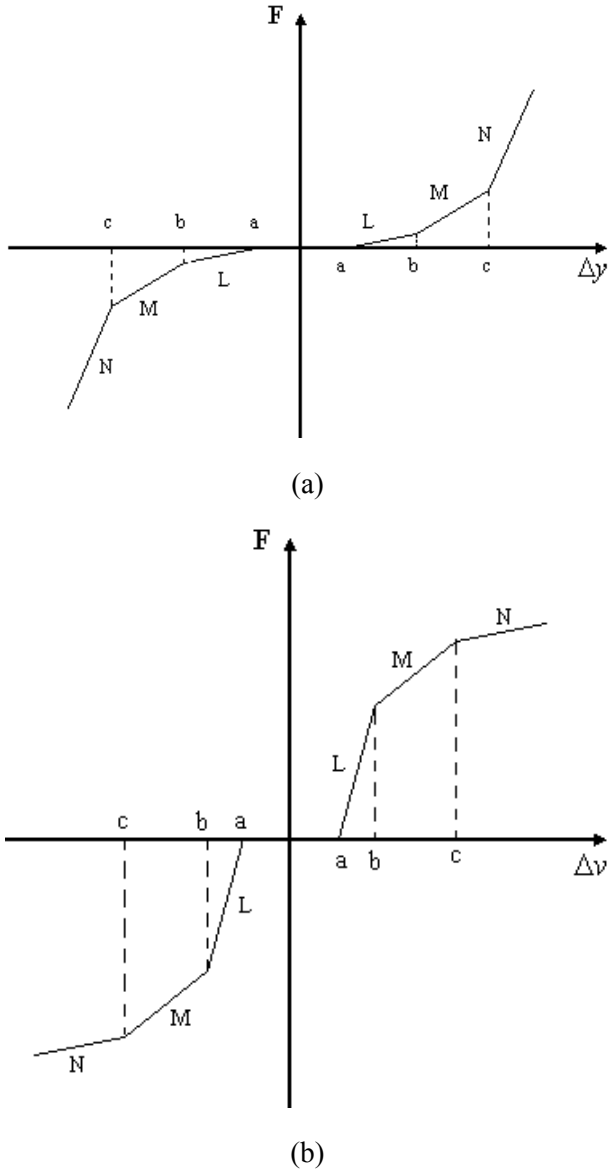

Figure 4. Suspension force characteristic: (a) Springs characteristic, (b) Dampers characteristic.

out force. The piecewise linear model of Figure 5-b makes it possible to approximate friction levels below break out during stationary conditions [16].

3. WHEELSET MODEL

As shown in Figures 2 and 3 wheelset has 6 DOF which is longitudinal, vertical and lateral movements, roll, yaw and axial rotations. The wheelset is connected to other parts of the wagon via primary suspension system. Contact between the wheels and rails is considered elastic. Unlike most previous works assuming single point contact, the present model uses multi point contact assumption for wheel-rail contact simulation. Multi point contact assumption increases model accuracy in simulation of wheelset lateral motion in derailment and curve passing.

To determine normal contact force between wheel and rail, relative position of wheel and rail must be determined at each instant. Using the coordinate of each wheel points in rail coordinate system, the penetration of wheel in rail can be determined [16].

The normal contact force is determined using Hertz contact theory. The force depends on the penetration at the contact point and the material properties of the wheel and the rail. In the evaluation of the normal contact force, a damping force is included in addition to the Hertzian component. The expression for the normal force used in this article is given by:

$$N = N_h + N_d = -K_h \delta^{3/2} - C\dot{\delta}|\delta| \quad (6)$$

Where δ is the indentation depth, N_h is the Hertzian (elastic) contact force, N_d is the damping force, K_h is the Hertzian constant and C is a damping constant [14].

Accurate determination of creep forces in wheel-rail contact point has a marked effect in wheelset simulation especially in derailment studies. In this article, the creep forces are determined using Kalker's nonlinear theory [17]. No linearization is used in the calculations of the creepages.

Nonlinear elements in wagon suspension,

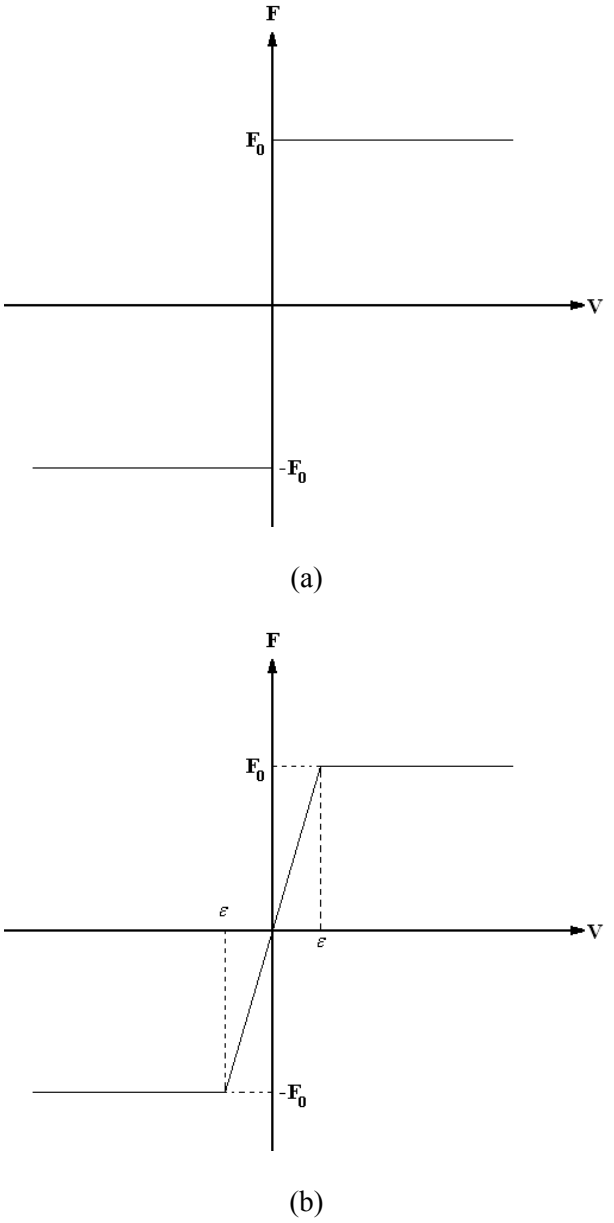

Figure 5. Coulomb friction element: (a) Ideal coulomb friction element, (b) Approximate coulomb friction element.

nonlinearity in determination of wheel-rail contact points and their normal and creep forces, makes the model fully nonlinear.

4. WHEEL AND RAIL PROFILES

Wheel and rail exact profiles are necessary for simulation of wheelset motion. In this article, wheel profile has been selected from the data in reference to [18]. Also, UIC Profil 60 has been used for rail profile [19].

5. IRREGULARITIES MODEL

Rail irregularities generally have a random distribution, and are considered as one of the major source of wagon vibration and wheelset derailment. The major causes of these irregularities are: incompatible substrate conditions, wheather conditions, rail age and excessive train commutation on rails [20].

The random rail irregularities are assumed to be stationary random and ergodic processes in space, with Gaussian amplitude probability densities and zero mean values. They are characterized by their respective one-sided power spectral density functions $G_{rr}(\omega)$ where ω is the route frequency. Fryba, et al [21] has summarized various commonly used power spectral density functions. In the present study, the power spectral density functions based on the results of measurements on US railway tracks is adopted, with the empirical formula for elevation of irregularities as:

$$G_{rr}(\omega)=\frac{A_v\,\omega_2^2(\omega^2+\omega_1^2)}{\omega^4(\omega^2+\omega_2^2)} \qquad (7)$$

Where $\omega_1 = 0.0233$ m^{-1} and $\omega_2 = 0.131$ m^{-1} and the parameter A_v is a coefficient related to line grade, as shown in Table 2.

TABLE 2. Coefficient for A_v.

Line Grade	A_v
1	15.52×10^{-8}
2	8.84×10^{-8}
3	4.91×10^{-8}
4	2.75×10^{-8}
5	1.55×10^{-8}
6	0.88×10^{-8}

A sample function of rail irregularities can be generated numerically using the following series:

$$r^d(x) = \sum_{k=1}^{N} a_k \cos(\omega_k x + \varphi_k) \quad (8)$$

Where a_k is the amplitude of the cosine wave, ω_k is a frequency within the interval $[\omega_l,\omega_u]$ in which the power spectral density function is defined, φ_k is a random phase angle with uniform probability distribution in the interval $[0,2\pi]$, x is the global coordinate measured from the start of the rail section and N is the total number of terms used to generate the rail irregularities function. The parameters a_k and ω_k are computed using Equations 9 and 10:

$$a_k = 2\sqrt{G_{rr}(\omega_k)\Delta\omega} \quad (9)$$

$$\omega_k = \omega_l + (k - \tfrac{1}{2})\Delta\omega \quad (10)$$

$$\Delta\omega = (\omega_u - \omega_l)/N \quad (11)$$

In which ω_u and ω_l are the upper and lower limits of the frequency, and N is a sufficiently large integer. These parameters are assumed, namely ω_u = 7.0 m^{-1}, ω_l = 0.01 m^{-1} and N = 2000.

Using Equations 7-11, random rail irregularities in each line grade can be generated. Typical samples of rail irregularities of American line grade 1, 4 and 6 produced by this method are shown in Figure 6. As shown in this figure, higher quality rails have irregularities with lower amplitude and their characteristic curve is smoother.

6. EQUATIONS OF MOTION

Three sets of coordinate systems are used to derive the equations of motion. The coordinate system $S_{x''y'''z'''}$ shown in Figure 2 has its origin at the track centerline with its x axis along rail centerline. The coordinate system $x''y''z''$ is an intermediate frame that is the $x'''y'''z'''$ rotated through an angle ψ about z''' axis. Then with a rotation φ about x'' axis, this coordinate system converts to coordinate system $x'y'z'$. The coordinate R_{xyz} has its origin at the center of mass of the part and it is made from rotation θ about the y' axis. The matrices of conversions of these coordinates are as follow:

$$\{P\}_S = [T^{\psi}][T^{\varphi}][T^{\theta}]\{P\}_R \quad (12)$$

In which:

$$[T^{\psi}] = \begin{bmatrix} \cos\psi & -\sin\psi & 0 \\ \sin\psi & \cos\psi & 0 \\ 0 & 0 & 1 \end{bmatrix} \quad (13a)$$

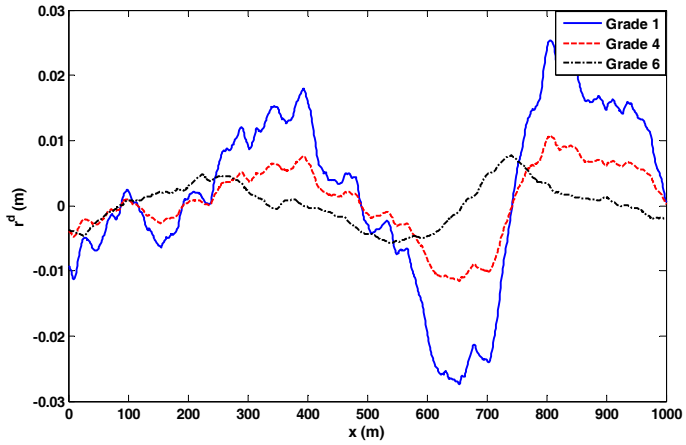

Figure 6. Samples of the railway track irregularities.

$$[T^{\varphi}]=\begin{bmatrix}1 & 0 & 0\\ 0 & \cos\varphi & -\sin\varphi\\ 0 & \sin\varphi & \cos\varphi\end{bmatrix} \quad (13b)$$

$$[T^{\theta}]=\begin{bmatrix}\cos\theta & 0 & \sin\theta\\ 0 & 1 & 0\\ -\sin\theta & 0 & \cos\theta\end{bmatrix} \quad (13c)$$

Using definition of coordinate systems, angular velocity of the part can be written as:

$$\Omega=\dot{\psi}\,k'''+\dot{\varphi}\,i''+\dot{\theta}\,j' \quad (14)$$

Using Equations 12 and 13 the angular velocity can be written in body coordinate system:

$$\Omega=(-\dot{\psi}\cos\varphi\sin\theta+\dot{\varphi}\cos\theta)\hat{i}+(\dot{\psi}\sin\varphi+\dot{\theta})\hat{j}+(\dot{\psi}\cos\varphi\cos\theta+\dot{\varphi}\sin\theta)\hat{k} \quad (15)$$

Because of axial symmetry of the wheelset, simpler coordinate systems can be used for deriving wheelset equation of motions. These coordinate systems and wheelset equations of motion are presented in reference [16].

For each part of wagon body, bolster and bogie equation of motion can be derived as follows [22]:

$$m\{\ddot{x}_c\}_S=\{F_x\}_S \quad (16a)$$

$$m\{\ddot{y}_c\}_S=\{F_y\}_S \quad (16b)$$

$$I_x\dot{\Omega}_x+(I_z-I_y)\Omega_y\Omega_z=\{M_x\}_R \quad (16d)$$

$$I_y\dot{\Omega}_y+(I_x-I_z)\Omega_x\Omega_z=\{M_y\}_R \quad (16e)$$

$$I_z\dot{\Omega}_z+(I_y-I_x)\Omega_x\Omega_y=\{M_z\}_R \quad (16f)$$

7. SIMULATIONS

In this section, solution of Equations 16 for all part of wagon is presented. These equations are solved using the Newmark-β method with time intervals of $\Delta t = 10^{-4}$ s. Wagon is moving on a rail with random irregularities. Wheelset derailment in different conditions is thereby investigated. Wagon parameters for dynamic simulation are presented in Table 3. Simulation is performed in wagon speed of 5, 20, 40, 80 and 100 m/s, and normal force, derailment coefficient and wagon body acceleration are computed in all cases. Simulation is performed in the following two cases:

- Similar vertical irregularities in right and left rails: In this case, longitudinal curves of the two rails are completely similar.
- Dissimilar vertical irregularities in right and left rails: in this case irregularities of right and left rails are from one grade, but their amplitude and phase are not necessarily similar.

7.1. Similar Irregularities in the Rails

Figures 7 and 8 illustrate simulation results for wagon speed 40 m/s with similar rail irregularities of grade 1 and grade 6. In this case, no lateral wheelset displacement exist, therefore, derailment coefficient does not vary significantly.

Variations of normal interaction force between wheel and rail for different speeds and line grades are shown in Figure 9. As seen in this figure, derailment coefficient increases with increase in train speed and rail irregularities. Using this figure and the criteria presented in Equation 4 maximum allowable vehicle speed for different line grades has been determined, and presented in Figure 15. The results released by FRA for track safety standards [23] are also shown in this figure.

Comparison of maximum allowable speed obtained from simulation with the data represented by FRA shows that the allowable values recommended by FRA are about 75 % of the values determined by simulation results for this type of wagon.

To study the effects of rail irregularities on ride comfort, vertical acceleration of wagon body moving on rails having different line grades is computed. As an example, Figures 7 and 8 show these accelerations in time and frequency domains for line grades 1 and 6.

Lei,et al and Noda, et al [8] have shown that vibrations in the frequency range of 5 to 8 Hz are undesirable for passenger ride comfort. Also the amplitude of wagon vibrations is an important

TABLE 3. Basic Dynamic Parameters of Wagon and Rail.

Notation	Parameter	Value
Wagon Body		
M_c	Wagon body mass	20000 kg
I_{cx}	Wagon mass moment of inertia about X axis	32268 kg m^2
I_{cy}	Wagon mass moment of inertia about Y axis	1125000 kg m^2
I_{cz}	Wagon mass moment of inertia about Z axis	1125000 kg m^2
Bolster		
M_{bol}	Bolster body mass	630 kg
I_{bolx}	Bolster mass moment of inertia about X axis	160 kg m^2
I_{boly}	Bolster mass moment of inertia about Y axis	100 kg m^2
I_{bolz}	Bolster mass moment of inertia about Z axis	160 kg m^2
Bogie		
M_{bog}	Bogie body mass	500 kg
I_{bogx}	Bogie mass moment of inertia about X axis	250 kg m^2
I_{bogy}	Bogie mass moment of inertia about Y axis	150 kg m^2
I_{bogz}	Bogie mass moment of inertia about Z axis	300 kg m^2
Wheelset		
M_w	Wheelset body mass	1180 kg
I_{wx}	Wheelset mass moment of inertia about X axis	680 kg m^2
I_{wy}	Wheelset mass moment of inertia about Y axis	73 kg m^2
I_{wz}	Wheelset mass moment of inertia about Z axis	680 kg m^2
r_w	Wheel radius	0.46 m
Rail		
G_r	Rail gage	1.435 m
η_r	Lateral rail slope	0.05 rad
θ_r	Longitudinal rail slope	0
Wagon Natural Frequencies		
f_1	The first natural frequency of wagon	6.44 Hz
f_2	The second natural frequency of wagon	8.14 Hz
F_3	The third natural frequency of wagon	42.29 Hz

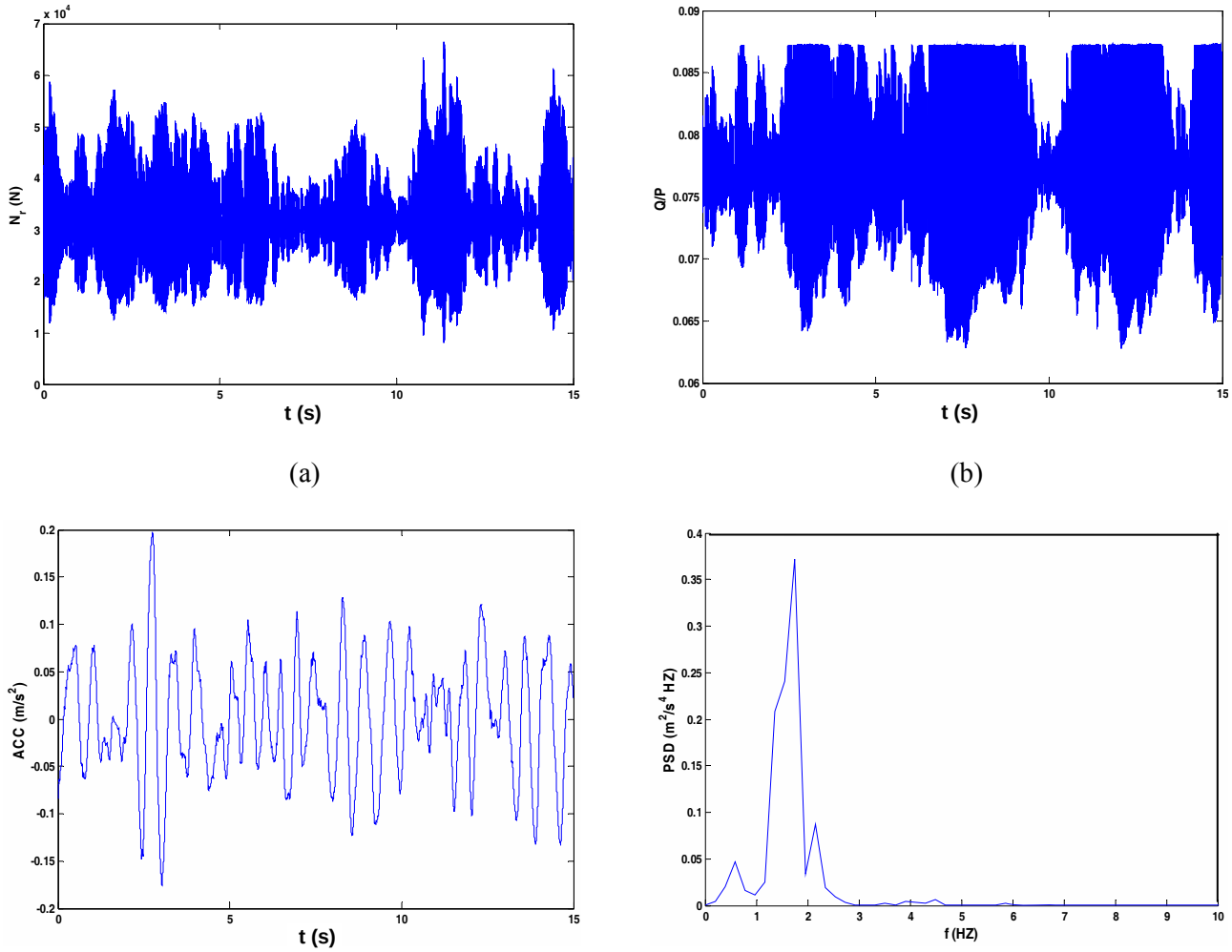

Figure 7. Simulation results for wagon speed 40 m/s and rail irregularities of grade 1 in the case of vertical similar irregularities in right and left rails.

parameters in passenger ride comfort. As shown in Figures 7 and 8 principal frequencies of wagon body vibrations for all cases are less than 2.5 HZ, but the amplitude of maximum vertical accelerations of the wagon body is very sensitive to irregularities of the track and train speeds, it increases with increased train speed and rail irregularities. This fact is illustrated in Figure 10.

7.2. Dissimilar Irregularities in Rails

Different factors cause dissimilar rail irregularities in right and left rails. Similar to previous section Figures 11 and 12 show simulation results for wagon speed of 40 m/s and rail irregularities of grade 1 and grade 6.

Comparing these figures with Figures 7 and 8 shows that in this case, normal force reduction in wheel-rail contact points is more, especially for low rail quality. Also, derailment coefficient in this case is more than the case with similar irregularities. For high train speeds and low quality rails, this coefficient exceed 0.8. As an example, when wagon moves with a speed of 100 m/s on a rail of grade 1, derailment coefficient rises to 1.4.

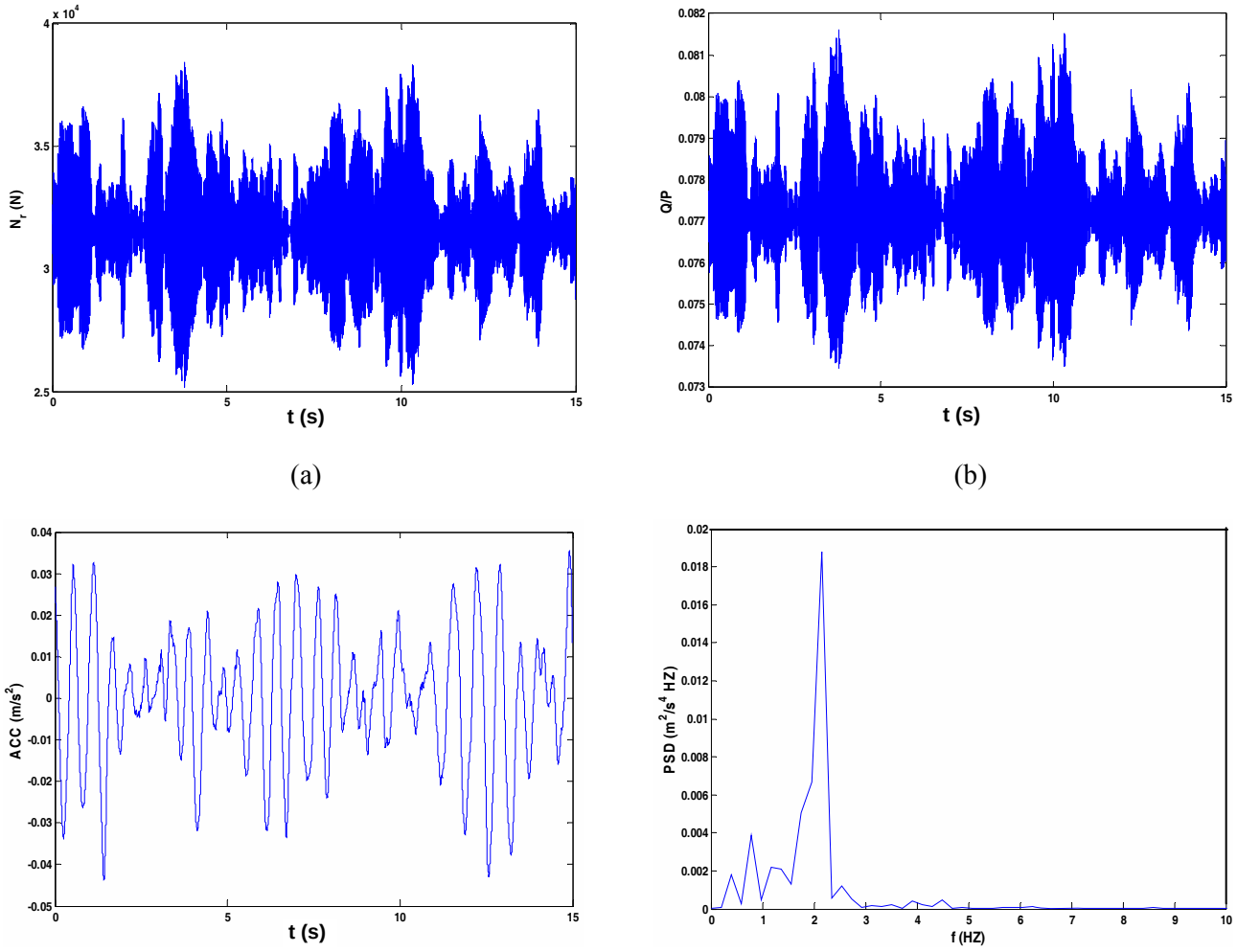

Figure 8. Simulation results for wagon speed 40 m/s and rail irregularities of grade 6 in the case of vertical similar irregularities in right and left rails.

Variations of normal interaction force between wheel and rail and derailment coefficient for different speeds and line grades are shown in Figure 13 and 14.

Using the results presented in Figures 13 and 14 and the criteria presented in Equations 4 and 5 maximum allowable vehicle speed for different line grade has been determined. The results are presented in Figure 15.

Comparing these results with the ones presented in last section shows that the wagons' safe speed determined by this method have more agreement with the FRA field test results.

Figures 11 and 12 indicate the wagon body lateral and vertical accelerations in time and frequency domain for line grades 1 and 6. As shown in these figures, principal frequencies of wagon body vibration in all cases are less than 2.5 HZ. Variation of amplitude of wagon body acceleration in vertical and lateral directions in different speeds and line grades are presented in Figures 16 and 17 respectively. As shown in these figures, the amplitude of maximum vertical and lateral accelerations of the wagon body increases with increase in train speed and rail irregularities. Therefore, the main reason for the reduction in ride

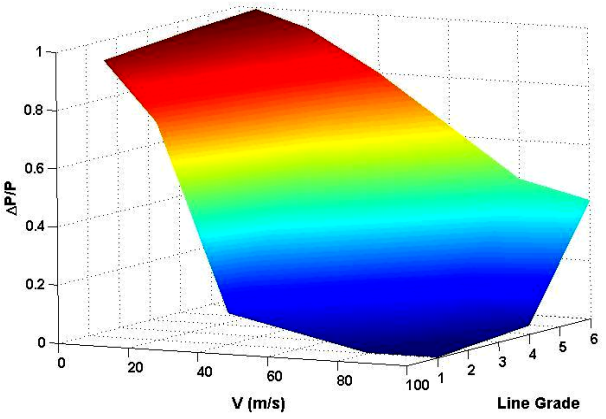

Figure 9. Ratio of interaction force reduction between wheel and rail in different speeds and line grades in the case of vertical similar irregularities in right and left rails.

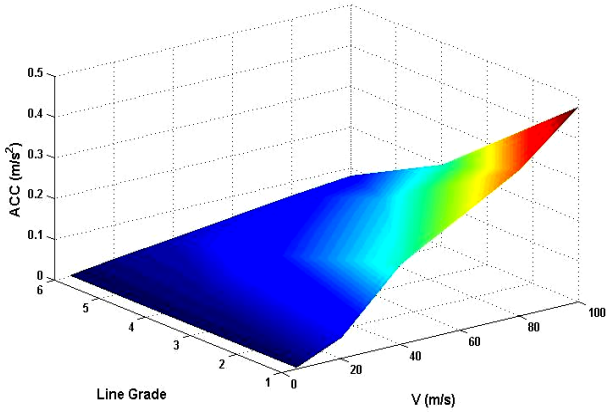

Figure 10. Amplitude of wagon body acceleration in different speeds and line grades in the case of vertical similar irregularities in right and left rails.

comfort will be the increased train speed and rail irregularities which increases the wagon vibration amplitude.

8. CONCLUSIONS

In this paper, a 3-D nonlinear model is used to simulate wagon movement on randomly irregular rail track. The simulation is performed for different wagon speeds and line quality.

Two cases are used to determine wagons' safe speed for different line grades. In the first case, rail irregularities are assumed to be similar in both rails and in second case, they are assumed to be dissimilar.

In the first case by investigating normal force reduction in wheel-rail contact points, wagon safe speed for different line grades is determined.

In the second case, besides normal force reduction in wheel-rail contact points, derailment coefficient is used to determine wagons' safe speed for different line grades.

Comparing these results with the results provided by FRA shows that, the assumption of dissimilar irregularities in rails lead to more precise results for wagons' safe speed.

To determine the effects of wagon speed and line quality on ride comfort, wagon acceleration in

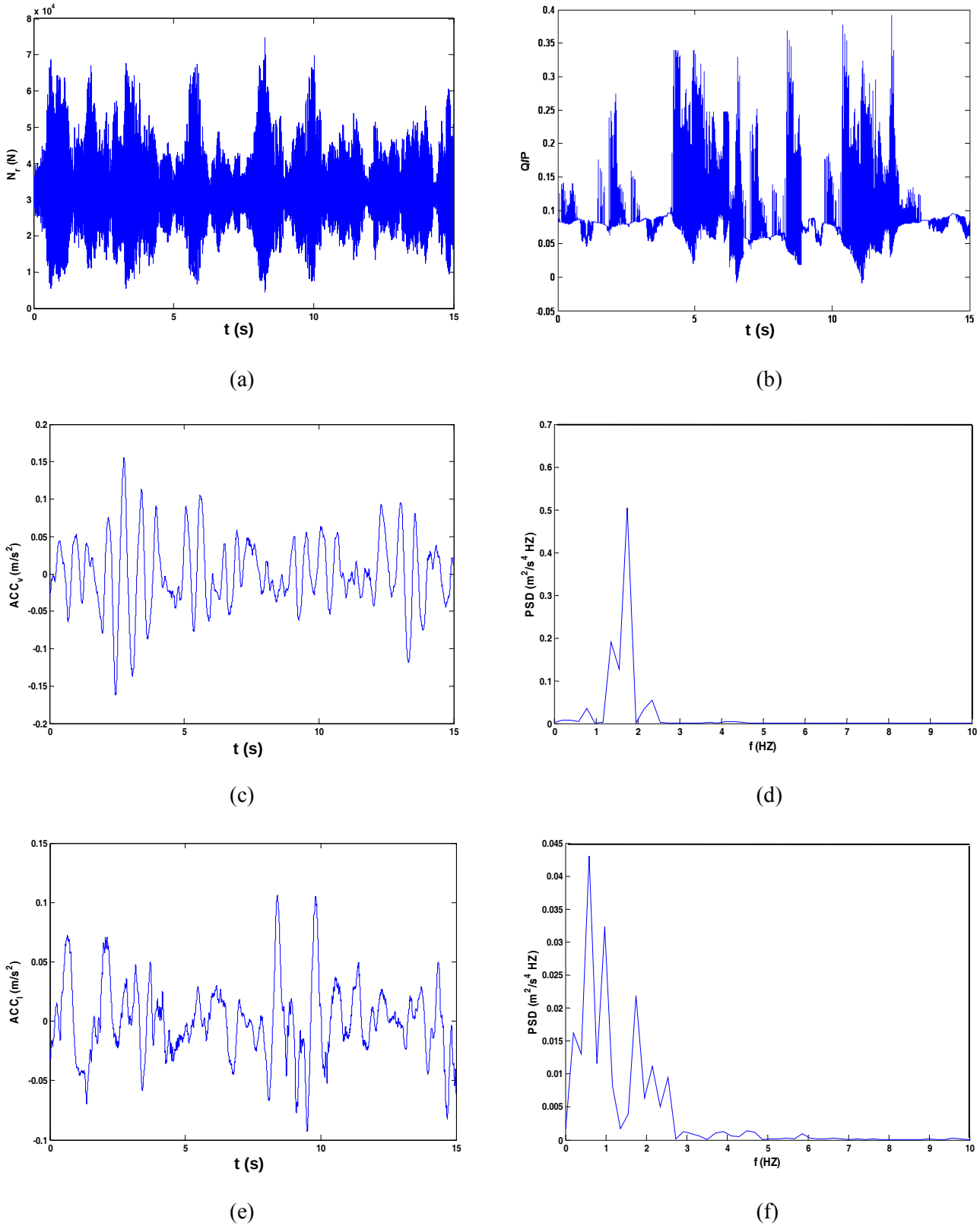

Figure 11. Simulation results for wagon speed 40 m/s and rail irregularities of grade 1 in the case of vertical dissimilar irregularities in right and left rails.

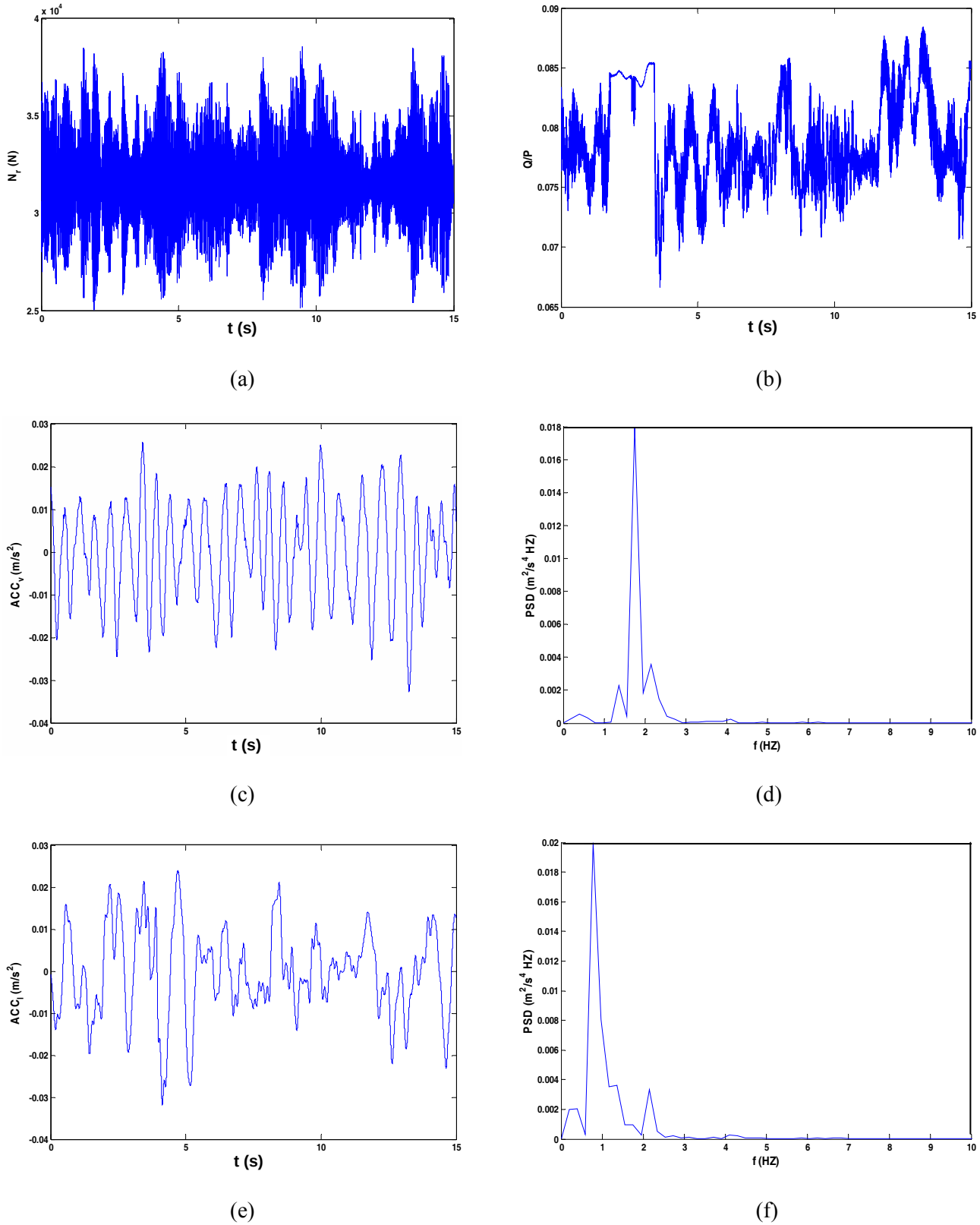

Figure 12. Simulation results for wagon speed 40 m/s and rail irregularities of grade 6 in the case of vertical dissimilar irregularities in right and left rails.

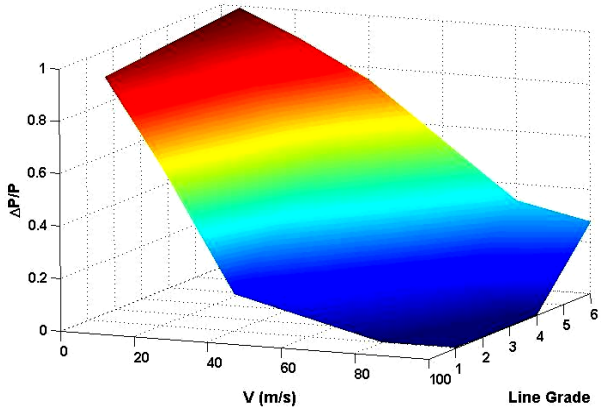

Figure 13. Ratio of interaction force reduction between wheel and rail in different speeds and line grades in the case of vertical dissimilar irregularities in right and left rails.

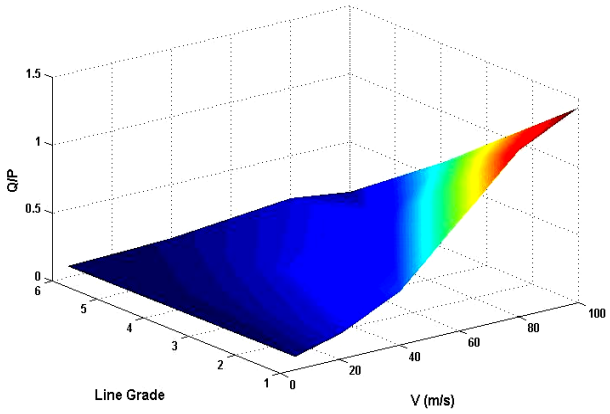

Figure 14. Maximum wheelset derailment coefficient in different speeds and line grades in the case of vertical dissimilar irregularities in right and left rails.

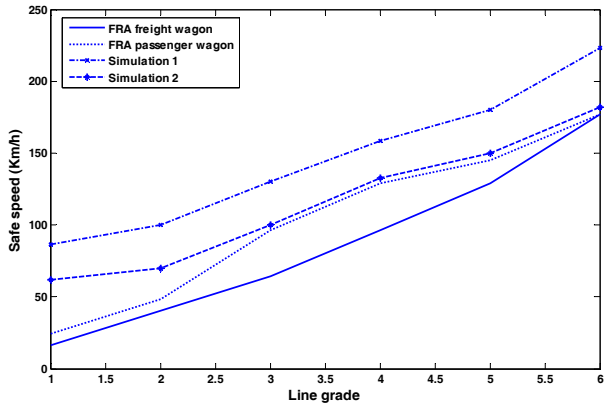

Figure 15. Wagon safe speed in different line grades.

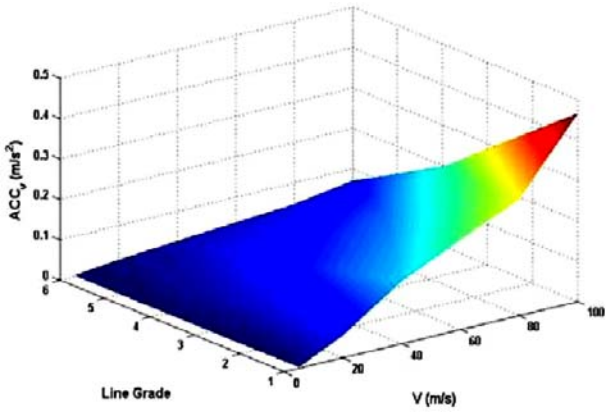

Figure 16. Amplitude of vertical acceleration of wagon body in different speeds and line grades in the case of vertical dissimilar irregularities in right and left rails.

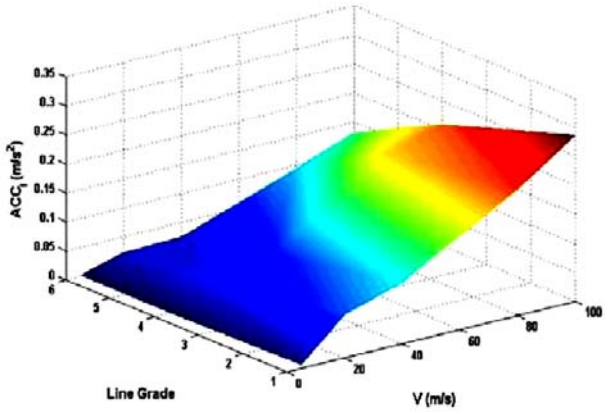

Figure 17. Amplitude of lateral acceleration of wagon body in different speeds and line grades in the case of vertical dissimilar irregularities in right and left rails.

time and frequency domain is computed in all cases. The simulation results show that the principal frequencies of wagon body vibration in all cases are less than 2.5 HZ, but the amplitude of maximum accelerations of the wagon body will increase with the increase in train speed and rail irregularities. Dominant vibration frequency in the range of 5 to 8 Hz has undesirable effects on passengers ride comfort. Therefore, the main reason for ride comfort reduction is the increase in train speed and rail irregularities will increase the wagon vibration amplitude.

9. REFERENCES

1. Matsuo, M., "Quasi-Static Derailment of a Wheelset", ***Quarterly Report of RTRI***, Vol. 27, No. 3, (1986), 94-97.
2. Jun, X. and Qingyuan, Z.,"A Study on Mechanical Mechanism of Train Derailment and Preventive Measures for Derailment", ***Vehicle System Dynamics***, Vol. 43, (2005), 121-147.
3. Elkins, J. A. and Carter, A., "Testing and Analysis Techniques for Safety Assessment of Rail Vehicles: The State of the Art", ***Vehicle System Dynamics***, Vol. 22, No. 3, (1993), 184-208.
4. Matsuura, A., "Dynamic Interaction of Vehicle and Track", ***Quarterly Report of RTRI***, Vol. 33, No. 1, (1992), 31-38.
5. Zhai, W. and Sun, X. "A Detailed Model for Investigating Vertical Interaction between Railway Vehicle and Track", ***Vehicle System Dynamics***, Vol. 23, (1994), 603-615.
6. Sun, Y. Q. and Dhanasekar, M., "A Dynamic Model for the Vertical Interaction of the Rail Track and Wagon System", ***International Journal of Solids and Structures***, Vol. 39, (2002), 1337-1359.
7. Au, F. T. K., Wang, J. J. and Cheung, Y. K., "Impact Study of Cable-Stayed Railway Bridges with Random Rail Irregularities", ***Journal of Engineering Structures***, Vol. 24, (2002), 529-541.
8. Lei, X. and Noda, N. A., "Analyses of Dynamic Response of Vehicle and Track Coupling System with Random Irregularity of Track Vertical Profile", ***Journal of Sound and Vibration***, Vol. 258, No. 1, (2002), 147-165.
9. Durali, M. and Jalili M. M., "Investigation on Dynamic Interaction Between Wagon and Randomly Irregular Rail Track", ***2005 ASME International Mechanical Engineering Congress and Exposition***, IMECE2005-80206, Orlando, Florida, U.S.A., (2005).
10. Durali, M. and Shadmehri, B., "Nonlinear Analysis of Train Derailment in Severe Braking", ***ASME Journal of Dynamic Systems, Measurement and Control***, Vol. 125, (2003), 48-53.
11. Durali, M. and Jalili, M. M., "Investigation of Train Dynamics in Passing through Curves Using a Full Model", ***2004 ASME/IEEE Joint Rail Conference***, RTD2004-66044, Baltimore, MD, U.S.A., (2004).
12. Ahmed, A., Shabana, M. B. and Jalili, R. S., "Numerical Procedure for the Simulation of Wheel/Rail Contact Dynamics", ***ASME Journal of Dynamic Systems, Measurement and Control***, Vol. 123, (2001), 168-178.
13. Zaazaa, Kh.-E. and Shabana, A. A., "Study of the Lateral Stability of Railroad Vehicle Systems using the Elastic Contact Approach", ***The Arabian Journal for Science and Engineering***, Vol. 29, No. 1C, (June 2004), 3-12.
14. Shabana, A. A., Zaazaa, Kh. E., Escalonab, J. L. and Sany, J. R., "Development of Elastic Force Model for Wheel/Rail Contact Problems", ***Journal of Sound and Vibration***, Vol. 269, (2004), 295-325.
15. Durali, M. and Jalili, M. M., "Investigation of the Effects of Rail Wear on Derailment of the Axle in Passing Over Rail Irregularities", ***The Third Asian Conference on Multibody Dynamics 2006***, ACMD 06-A00612, Komaba, Tokyo, Japan, (August 1-4, 2006).
16. Garg, V. K. and Dukkipati, R. V., "Dynamics of Railway Vehicle Systems", Canada Academic Press, Canada, (1984).
17. Kalker, J. J., "Three-Dimensional Elastic Bodies in Rolling Contact", Kluwer Academic Publishers, Dordrecht, Boston, London, U.K., (1990).
18. "UIC Leaflet 510-2: Conditions Concerning the Use of Wheels of Various Diameters", The International Union of Railways, 4th Edition, (2004).
19. "UIC Leaflet 861-3: Standard 60 kg/m Rail Profiles-Types UIC 60 and 60E", The International Union of Railways, 3rd Edition (2002).
20. Iyengar, R. N. and Jaiswal, O. R., "Random Field Modeling of Railway Track Irregularities", ***Journal of Transportation Engineering***, (July/August 1995), 303-308.
21. Fryba, L., "Dynamics of Railway Bridges", Thomas Telford, London, U.K., (1996).
22. D'Souza A. F. and Garg, V. K., "Advanced Dynamics, Modeling and Analysis", Prentice Hall, Newjersey, U.S.A., (1984).
23. Federal Railway Administration, "Track Safety Standards", U. S. Department of Transportation, Office of Safety Research, Washington, U.S.A., (March 1975).